# Majority of choice-related variability in perceptual decisions is present in early sensory cortex

Charles A. Michelson[1], Jonathan W. Pillow[2] and Eyal Seidemann[1]

[1]Institute for Neuroscience, Center for Perceptual Systems, Departments of Psychology and Neuroscience, University of Texas at Austin

[2]Princeton Neuroscience Institute, Department of Psychology, Princeton University

**ABSTRACT**

**While performing challenging perceptual tasks such as detecting a barely visible target, our perceptual reports vary across presentations of identical stimuli. This perceptual variability is presumably caused by neural variability in our brains. How much of the neural variability that correlates with the perceptual variability is present in the primary visual cortex (V1), the first cortical processing stage of visual information? To address this question, we recorded neural population responses from V1 using voltage-sensitive dye imaging while monkeys performed a challenging reaction-time visual detection task. We found that V1 responses in the period leading to the decision correspond more closely to the monkey's report than to the visual stimulus. These results, together with a simple computational model that allows one to quantify the captured choice-related variability, suggest that most this variability is present in V1, and that areas outside of V1 contain relatively little independent choice-related variability.**

**IMPACT**

This study uses a combination of cortical imaging from monkeys performing a challenging visual detection task and a simple computational model to show that the majority of the neural variability that correlates with the monkey's variable behavioral choices is present in the primary visual cortex.

## INTRODUCTION

When we perform a challenging perceptual task, what fraction of the neural variability that relates to our variable perceptual decisions is present in early sensory cortex? One way to address this fundamental question is to measure neuronal activity in a relevant sensory cortical area during the temporal interval over which the decision is formed and assess the extent to which the measured activity is correlated with trial-to-trial variability in perceptual decisions. If such measurements are highly predictive of behavioral choice, then most choice-related variability must be present in this sensory area. This result would imply that other areas contain little choice-related variability that is independent of the variability present in the sensory area.

Previous studies of the relationship between neural and behavioral variability have discovered co-variations between responses of individual neurons in sensory cortex and a subject's behavioral choices to repeated presentations of an identical near-threshold sensory stimulus (e.g., (Britten et al 1996, Celebrini & Newsome 1994, Cook & Maunsell 2002, de Lafuente & Romo 2005, Dodd et al 2001, Nienborg & Cumming 2006, Nienborg & Cumming 2009, Palmer et al 2007, Purushothaman & Bradley 2005, Uka & DeAngelis 2004). These co-variations, however, tend to be very weak, implying that individual neurons capture only a small fraction of the neural variability related to decisions. The large amount of choice-related variability that is unaccounted for in single-neuron studies may be distributed across other (unmeasured) sensory neurons, and may also occur outside of the sensory area. Even if the majority of choice-related variability occurred in a

distributed sensory cortical population, single neurons still may not provide strong predictions of choice because sensory neurons are only weakly correlated with one another (e.g.,(Zohary et al 1994)), and therefore, one neuron's responses are only weakly related to the population response. Thus, single-neuron studies cannot provide strong constraints on whether most decision-related neural variability is present in sensory cortex.

In contrast, methods for measuring neural population responses, such as voltage-sensitive dye imaging (VSDI) (Grinvald & Hildesheim 2004), have the potential to provide stronger constraints by capturing a larger fraction of the choice-related variability within the sensory area. Because even simple, spatially localized stimuli evoke responses over a broad region of sensory cortex (Chen et al 2006, Grinvald et al 1994, Palmer et al 2011), and because these sensory cortical neurons are only weakly correlated with one another, subjects can benefit from combining these distributed signals to inform decisions. Thus, perceptual decisions may be based on the combined activity from a large population of sensory neurons. In this case, population measures may show stronger co-variations with choice, and thus account for a greater fraction of the choice-related neural variability. However, such methods are likely to also contain various sources of variability unrelated to choice, such as choice-irrelevant neural variability and measurement noise, which can weaken the relationship between the measured neural activity and behavior.

To address the possibility that choice-related activity is distributed across many sensory neurons, we used VSDI to record from a large population of neurons in primary visual cortex (V1) of two monkeys while they performed a difficult visual

detection task. We placed the visual target so that it fell at the center of the visual area represented by the imaged neurons. We assume that the stimulus-related signals that the monkey uses to form decisions in our task pass through the area that we are imaging in V1. In other words, V1 provides the sensory evidence, and we can eavesdrop on this evidence while the monkey forms a decision. We further assume that there is a point in time in each trial when the monkey commits to a choice. In order for the monkey to perform the task at above chance, this decision point must be delayed by at least several tens of ms from the response latency in V1. We focus on analyzing V1 signals during this brief pre-decisional period.

V1 signals during the pre-decisional period are variable, and this variability in the evidence must affect the monkey's choices. The sources of this pre-decisional variability are unknown. Some of this variability is likely to be due to feedforward sources and some of it is likely to be due to feedback. Our goal here is not to distinguish between, or quantify, these two sources, but rather to quantify the total pre-decisional choice-related variability present in V1, irrespective of its source. Additional sources of variability downstream to V1 that affect choice but are not relayed to V1 prior to the decision are likely to exist. Our goal is to determine if the majority of the pre-decisional choice-related variability is present in V1. This is a fundamental question to which the answer is currently unknown.

To better understand the relationship between measurements of neural variability and perceptual decisions, we developed a simple computational model. This model is advantageous over previous methods, because it can be used to quantify the fraction of choice-related variability captured in a measurement of

neural population responses independent of choice-unrelated variability. Together, this approach allows us to determine a lower bound on the fraction of choice-related variability that occurs in V1 during performance of a detection task.

## RESULTS

*Choice-related population activity in macaque V1*

We trained two monkeys to perform a simple reaction-time visual detection task (Fig. 1B). The monkey began each trial by directing gaze to a central fixation point. To obtain a reward, the monkey had to rapidly shift gaze to a small peripheral target during 'target-present' trials (50% of trials), or to maintain fixation on the central fixation point during 'target-absent' trials (the remaining trials). We used a small Gabor patch stimulus (sinusoidal grating in a 2-D Gaussian envelope) to effectively drive V1 cells, and presented the stimulus at one or two contrast levels near each monkey's perceptual detection threshold to maintain task difficulty. Target-present trials were classified as 'Hits' if the monkey correctly detected the target and 'Misses' otherwise. Target-absent trials were classified as 'False Alarms' (FAs) if the monkey reported seeing a target and 'Correct Rejects' (CRs) otherwise (Fig. 1C; Supplemental Table S1).

While the monkeys performed the task, we used voltage-sensitive dye imaging (VSDI) to measure population responses from V1, an area likely to play a central role in performance of such tasks. VSDI measures changes in membrane potential from large populations of neurons with a dominant contribution from layer 2/3 (Chen et al 2012, Petersen et al 2003). Previous work showed that this

technique can be sufficiently sensitive to outperform monkeys in a similar detection task when combining single-trial VSDI signals optimally (Chen et al 2006, Chen et al 2008). Furthermore, because V1 contains a topographic map of visual space, the target activates a limited region in V1 (Chen et al 2006, Sit et al 2009), and this region can be precisely localized and entirely captured by VSDI. Thus, VSDI may be capable of capturing a large portion of choice-related variability in V1.

What are the expected trial-to-trial co-variations between VSDI responses and the monkey's choices? Consider a scenario in which all choice-related variability is present in V1 during a detection task. Intuitively, in this case, FA responses should resemble the average target-evoked responses, with amplitudes that exceed the internal detection criterion, even though the target is absent. Similarly, Miss responses should fall below the internal detection criterion, even though the target is present. Thus, in this case, we expect the average V1 responses on FAs to exceed responses on Misses. On the other hand, if most of the choice-related variability occurs downstream to V1, V1 responses should be only weakly correlated with choice, and the average responses in FAs should be much weaker than in Misses.

Results from a representative VSDI experiment (Fig. 2A) reveal large choice-related modulations at the level of neural populations in V1. On average, the stimulus evoked a broad Gaussian-shaped response across the population of neurons, consistent with our previous results (Chen et al 2006, Chen et al 2008, Chen & Seidemann 2012, Sit et al 2009). The mean stimulus-present and -absent maps were each further partitioned into mean Hit and Miss maps, and mean FA and

CR maps, respectively. These maps reveal robust choice-related differences. Similar choice-related activity is also observed in the grand average results combined across all of our data sets (Fig. 2B; see Fig. 2 Supplementary Fig. 1 for results from individual monkeys). These maps show that choice-related activity, as revealed by the Hit-Miss and FA-CR difference maps, is distributed broadly across the neuronal population rather than being restricted to a small region. To quantify these choice-related differences, we computed the amplitude of the response in each trial (Fig. 2C). Average amplitudes are significantly larger in Hits than in Misses ($p<0.001$, bootstrap test), significantly larger in FAs than in CRs ($p<0.001$, bootstrap test), and significantly larger in FAs than in Misses ($p=0.009$), suggesting that in this task the population activity in V1 corresponds more closely to the subject's choice than to the stimulus.

*Computational model for assessing the fraction of choice-related variability in V1*

Our results show significant choice-related variability in V1 but cannot, by themselves, determine whether most of the choice related variability is present in V1. To address this question, we developed a simple computational model of the pooled single-trial VSDI responses and used this model to obtain a quantitative estimate of the fraction of choice-related variability present in V1. In our model, the pooled sensory signal in target-absent and target-present trials is assumed to be normally distributed with variance $\sigma_s^2$ and means zero and one, respectively (Fig. 3, 'S'). During formation of the decision, additional *independent* decision-related Gaussian noise with variance $\sigma_d^2$ is added to the pooled sensory response (Fig. 3,

'D'). The total decision variability, which controls the subject's accuracy, is thus the sum of the contributions from these two independent sources of decision-related variability, $\sigma_{td}^2 = \sigma_s^2 + \sigma_d^2$. Note that this formulation does not distinguish among the various possible sources of the pre-decisional choice-related V1 variability. Thus, σs2 could have bottom-up (feedforward) and top-down (feedback) contributions, while σd2 captures choice-related variability outside of V1 that is independent of V1 variability and is therefore inaccessible form V1 measurements.

The subject reports 'target present' if the decision variable exceeds a criterion, and 'target absent' otherwise. As experimenters, we have access to the sensory neural responses (Fig. 3, 'S'), but we assume that our measurements are mixed with independent, choice-unrelated noise with variance $\sigma_m^2$ (Fig. 3, 'M') which combines neural and non-neural sources of variability. The total variability in the measured signal thus includes both the sensory variability and the variability in the choice-unrelated noise, $\sigma_{tm}^2 = \sigma_s^2 + \sigma_m^2$. Here we employ a slightly richer model that takes into account multiple target contrasts and experiment-to-experiment variations in VSDI signal quality (see Methods).

Our model can be used to estimate the fraction of the total decision-related variability that is present in the sensory area, $\sigma_s^2 / \sigma_{td}^2$, which we abbreviate DF ('decision fraction'). A second quantity of interest is the fraction of the total measured variability that is choice-related, $\sigma_s^2 / \sigma_{tm}^2$, which we abbreviate MF ('measurement fraction'). Consistent with our intuition, the model's behavior shows that the difference between the mean response in FAs and Misses is directly related

to DF. When DF is high, the mean FA exceeds the mean Miss (Fig. 4A, dashed red vs. dashed blue arrows). When DF is low, the mean Miss exceeds the mean FA (Fig. 4C), and the two means are equal at some intermediate value of DF. In fact, there is a linear relationship between the difference in these means and DF (Fig. 4E, black curve). In addition, as DF decreases, the correlation between the measured response and choice drops. A common metric for measuring this correlation is choice probability (CP), which measures the discriminability of two distributions of neuronal responses that belong to the same stimulus condition but to two different behavioral choices, such as 'Hits' (solid blue line) and 'Misses' (dashed blue line). As DF decreases, CP drops from a value of 1 (perfect discriminability) toward 0.5 (no discriminability) (Fig. 4E, gray curve). Importantly, while CP is strongly affected by measured variability that is choice unrelated (Fig. 4D,F), such variability has no effect on the means of the responses tied to each of the 4 behavioral outcomes. The invariance of the means with choice-unrelated variability allows our model to estimate DF independent of MF.

By applying our model to our results, we found that the majority of choice-related variability is present in V1. To estimate the fraction of choice-related variability captured by our VSDI measurements, we combined the signals over space and time into a single value for each trial, and examined the distribution of these scalar responses across trials. We first consider results under a simple pooling rule that uses weights proportional to the average choice-triggered responses (see Methods). The mean pooled signal is significantly higher in FA than in Miss trials, consistent with Fig. 2C. According to our model, these means imply that DF = 0.77

(95% CI: [0.56 1.0]), or in other words, 77% of the choice-related variability is present in V1. Similar results were obtained with a wide range of plausible candidate spatial pooling rules (Table 1), providing evidence that in our task, the majority of choice related activity is present in V1.

*Effect of partial overlap between subject and researcher's sensory neural pools*

Our model (Fig. 3) assumes that the subject and researcher share equal access to the V1 population. However, population measures such as VSDI are limited to finite spatial extent, spatial resolution, and cortical depth. Thus the subject and researcher's pooled sensory responses may overlap only partially. To explore the possible impact of partial overlap, we extended our model by simulating V1 as a 2-dimensional patch of neurons/pixels with signal and noise characteristics that matched those from the real data (see Supplemental Methods). We then performed simulated experiments in which the researcher, the subject, or both, are given independent access only to a random sub-population of the simulated cortex. Our results (Fig. 5) show that the DF estimated by our model is a *lower bound* on the true fraction of choice-related variability present in sensory cortex, because some of what our model considers as downstream noise may actually reside in V1.

*Dynamics of choice-related variability in V1*

Are the choice-related signals reported here pre-decisional or post-decisional? V1 responses to small stimuli at near-threshold contrast have long latencies and build up slowly (Sit et al 2009). Therefore, it seems unlikely that the choice-related signals

reported here reflect post-decisional top-down modulations, at least during the first ~100 ms after response onset (though they could reflect pre-decisional top-down signals). Nevertheless, to assess possible contribution of post-decisional top-down signals to our results, we compared the dynamics of the choice-related signals to the dynamics of the stimulus-evoked responses (Fig. 6). If the choice-related differences we observe were the result of a feedback signal that reflects a decision that had already been formed, we would expect choice-related signals to be delayed relative to the stimulus evoked response. Instead, the choice-related signals emerge at the same time as the evoked response and have similar dynamics. The near correspondence between the onset and dynamics of the choice-related signals and that of the stimulus-evoked response suggests that the choice-related signals are not the consequence of a decision that has already been formed and are therefore pre-decisional.

Additional analysis of eye position suggests that our results are not due to small variations in eye movements (Supplemental Table S2).

## DISCUSSION

Here we present two main findings. First, in a visual detection task, there is strong choice-related activity in V1 that is distributed across tens of $mm^2$ of cortex. This finding suggests that subjects combine sensory signals from a broad region of cortical space in order to inform decisions. Second, V1 population responses correspond more closely to the subject's choices than to the stimulus. To estimate the fraction of choice-related variability present in V1, we developed a simple model for studying the relationship between choice-related activity and noisy measures of neural population responses. Applying this model to our data, we find that V1 population responses account for the majority of the subjects' choice-related neural variability. Our results are consistent with previous studies that used indirect methods to infer the sources of behavioral variability (Brunton et al 2013, Osborne et al 2005), and with recent studies arguing that correlated noise present in early sensory areas is the primary factor limiting perception (Moreno-Bote et al 2014, Pitkow et al 2015).

The choice-related signals we observed are likely to contribute to the decision and limit behavior because they co-occur in space (Fig. 2) and in time (Fig. 6) with the V1 signals that the subject must use in order to perform the task. In other words, to perform our detection task, monkeys must rely on signals that pass through the imaged area in V1 during a brief pre-decisional temporal interval. These pre-decisional V1 signals are variable, and this variability must therefore affect the monkeys' decision. The sources of the V1 variability that affect decisions are not known, and are likely to include feedforward and feedback contributions. While

feedback contributions to choice-related activity are well documented (e.g., (Nienborg & Cumming 2009)), their relative contribution to pre-decisional sensory signals is unknown. A major open question is whether additional sources of independent variability outside of V1 (e.g., variability in decision and motor planning areas which is not relayed back to V1 prior to the decision), could be a major source of the variability that limits behavior. Our results provide novel evidence against this possibility, and suggest that most of the variability that limits performance in detection tasks is present in V1.

What might be the sources of the pre-decisional V1 variability? Because the stimulus sequence in our task was random, top-down signals that add a variable bias to V1 activity (e.g., signals reflecting trial-by-trial expectations) would be detrimental to task performance. Since our results were obtained from highly trained subjects, the presence of such detrimental top-down signals in our results is likely to have been minimized. Another potential source of top-down variability in V1 is fluctuations in spatial attention. In a recent study of spatial attention in V1 which employed a similar detection task with similar temporal cueing (a change in fixation point brightness 300 ms before the time of target onset), we observed attentional effects that precede stimulus onset and spread over a much larger spatial extent than the stimulus-evoked responses (Chen & Seidemann 2012). Thus, these top-down attentional signals appear to have different spatiotemporal dynamics from the choice-related responses observed here (Fig. 2D; Fig. 6). Finally, attention and alertness have been reported to have a multiplicative effect on sensory responses (Reynolds & Heeger 2009). Such multiplicative effects are less

likely to account for the signals that we observed in FA trials in which no sensory stimulus was present. These considerations suggest that in our task, trial-by-trial fluctuations in attention and alertness may have a relatively small contribution to pre-decisional choice-related variability in V1. Fluctuations in attention and alertness might instead contribute primarily to V1 variability that is not limiting performance (Moreno-Bote et al 2014, Pitkow et al 2015) and is therefore choice unrelated.

Regardless of its origin, we show here that in a detection task, the majority of choice-related variability can be found in V1 during the epoch leading to the decision, and that this variability has spatiotemporal dynamics similar to those of the target-evoked response. These results provide strong constraints on models that link neural responses in early sensory cortex and perceptual decisions.

Our result that the sensory population signals correspond more closely to the subject's choices than to the stimulus is similar to findings reported previously in human V1 by fMRI (Ress & Heeger 2003). However, due to the sluggish nature of fMRI signals and the delayed-response task design, the previous study was unable to determine whether the choice-related activity observed in sensory cortex occurred before or after the subject's decision. The previous study found similar activity in Hits and FAs and similar activity in Misses and CRs, suggesting that the previous results were dominated by activity occurring in an epoch in which stimulus-related signals had already vanished. In contrast to the slow and indirect nature of the fMRI signal, the fast temporal dynamics of the voltage-sensitive dyes and our reaction-

time task design allowed us to focus on choice-related signals that occur before the decision.

Our study speaks to fundamental questions about the relationship between noisy sensory representations and perceptual decisions. Here we show that decision-related neural activity is distributed broadly in early sensory cortex, suggesting that subjects pool information over a large population of sensory neurons to inform decisions, rather than relying on a small group of highly informative neurons. Second, we provide evidence that most choice-related neural variability is already present in early sensory cortex prior to the decision, suggesting that downstream circuits add little independent variability that affects decisions. An important goal for future studies is to determine the extent to which these results hold in other visual perceptual tasks and in other sensory modalities, and to explore the origins of this pre-decisional choice-related activity.

## MATERIALS AND METHODS

All procedures were approved by the University of Texas Institutional Animal Care and Use Committee and conformed to NIH standards. Two monkeys were trained to perform a reaction-time visual detection task. While each monkey performed the task, we recorded neural population signals in V1 using the voltage-sensitive dyes RH-1838 or RH-1691 (Shoham et al 1999). Imaging data were obtained using an Imager 3001 system (Optical Imaging, Inc.), collected at a resolution of 512x512 pixels at a sampling rate of 100 Hz. Similar task and VSDI processing methods have been described previously (Chen et al 2006, Chen et al 2008).

In order to understand the relationship between measurements of population neural activity in primary visual cortex and behavioral choice, we developed a simple model, outlined in Fig. 3. Detailed description of our model derivations and maximum likelihood calculation is given in Supplemental Information. Briefly, we start with the assumption of three independent Gaussian, additive noise sources: sensory noise $n_s$; downstream decision-related noise $n_d$; and decision-unrelated noise affecting the VSDI measurements $n_m$. We have previously shown that VSDI signals are consistent with Gaussian additive noise (Chen et al 2006) and we performed similar tests to verify these properties in our present data (see Fig. 7). We assume these noise sources to be zero-mean Gaussians with variances $\sigma_s^2$, $\sigma_d^2$ and $\sigma_m^2$, respectively. The subject's internal decision variable is $R_d = X + n_s + n_d$, where $X = \{0, c\}$ represents the strength of the visual stimulus

response and takes on the value 0 when the target is absent, or the value c when the target is present. Because the target was limited to a narrow range of contrasts (2.6%-5.0%), we fit a line to the aggregate data across all threshold target-present contrast levels and all experiments to determine how c depends on target contrast. We model the pooled response measured by the experimenters as $R_m = \kappa(X + n_s) + n_m$ where $\kappa$ represents the dye sensitivity, which determines how strongly V1 activity modulates the VSDI signal and was estimated based on the average amplitude of the response to 25% contrast targets in a control block immediately prior to each detection block. Dye sensitivity varies across experiments due to fluctuations in the quality of staining. The subject's binary decision $D$ is determined by a threshold, $D = H(R_d - t)$ where $H(\cdot)$ is the Heaviside step function and t is the criterion. Given these ingredients, the log probability of the subject's decision $D$ and the observed outcomes $R_m$ on a single trial is given by:

$$\log P(D, R_m \mid X, \theta) = \sum_{j=1}^{N} [(1 - D_j)\log \Phi(z_j) + D_j \log(1 - \Phi(z_j)) - \frac{(\kappa X_j - R_{mj})^2}{2\sigma_{tm}^2} - \log \sigma_{tm}] \quad (1)$$

plus a constant that does not depend on the model parameters, where

$$z_j = \frac{t - X_j(1 - \alpha\kappa^2) - \alpha\kappa R_{mj}}{\sqrt{\sigma_{td}^2 - \alpha\kappa^2\sigma_s^2}} \quad (2)$$

and where $D \in \{0,1\}$ is a binary variable that represents whether or not the subject reported seeing the target , $t$ is the subject's criterion, $\Phi(\cdot)$ is the standard normal cumulative density function (cdf), $\sigma_{tm}^2 = \kappa^2\sigma_s^2 + \sigma_m^2$ is the total measurement noise variance, $\sigma_{td}^2 = \sigma_s^2 + \sigma_d^2$ is the total decision noise variance, and $\alpha = \sigma_s^2 / \sigma_{tm}^2$ is the

ratio of shared to total measurement noise variance. We obtained maximum likelihood fits of the model parameters $\theta = \{\sigma_m^2, \sigma_d^2, \sigma_s^2, t, \kappa\}$ by numerical optimization of the log-likelihood (given by Eq. 1, summed over all trials) using MATLAB's `fmincon`.

While DF and MF values were obtained from parameters estimated by the full model (Eq. 1) that takes into account variations in contrast and experiment-to-experiment fluctuations in signal quality, such variations lead to a broadening of the distributions of scalar responses tied to each behavioral category. For this reason we used a simplified model with a single contrast value and no variations in VSDI signal quality (Fig. 3) to illustrate our results (Fig. 4). In the simplified model, $\bar{R}_{FA} - \bar{R}_M$ has a linear relationship with DF once the total decision-related variability is fixed (Fig.4E):

$$E[R_m \mid FA] - E[R_m \mid Miss] = \frac{\sigma_s^2}{\sigma_{td}}\left(\psi\left(\frac{-t}{\sigma_{td}}\right) + \psi\left(\frac{t-1}{\sigma_{td}}\right)\right) - 1, \qquad (3)$$

where $\psi(\cdot) = \phi(\cdot)/\Phi(\cdot)$ is the ratio of standard normal pdf to cdf.

**Acknowledgements**

We thank Tihomir Cakic, Yuzhi Chen and other members of the Seidemann laboratory for their contributions to this project. This work was supported by NIH/NEI RO1EY016454 and RO1EY16752 (ES) and a Ruth L. Kirschstein NRSA (CAM).

## References


Britten KH, Newsome WT, Shadlen MN, Celebrini S, Movshon JA. 1996. A relationship between behavioral choice and the visual responses of neurons in macaque MT. *Vis Neurosci* 13: 87-100

Brunton BW, Botvinick MM, Brody CD. 2013. Rats and humans can optimally accumulate evidence for decision-making. *Science* 340: 95-8

Celebrini S, Newsome WT. 1994. Neuronal and psychophysical sensitivity to motion signals in extrastriate area MST of the macaque monkey. *J Neurosci* 14: 4109-24

Chen Y, Geisler WS, Seidemann E. 2006. Optimal decoding of correlated neural population responses in the primate visual cortex. *Nat Neurosci* 9: 1412-20

Chen Y, Geisler WS, Seidemann E. 2008. Optimal temporal decoding of neural population responses in a reaction-time visual detection task. *J Neurophysiol* 99: 1366-79

Chen Y, Seidemann E. 2012. Attentional modulations related to spatial gating but not to allocation of limited resources in primate V1. *Neuron*

Cook EP, Maunsell JHR. 2002. Dynamics of neuronal responses in macaque MT and VIP during motion detection. *Nature Neuroscience* 5: 985-94

de Lafuente V, Romo R. 2005. Neuronal correlates of subjective sensory experience. *Nature Neuroscience* 8: 1698-703

Dodd JV, Krug K, Cumming BG, Parker AJ. 2001. Perceptually bistable three-dimensional figures evoke high choice probabilities in cortical area MT. *J Neurosci* 21: 4809-21

Grinvald A, Hildesheim R. 2004. VSDI: a new era in functional imaging of cortical dynamics. *Nat Rev Neurosci* 5: 874-85

Grinvald A, Lieke EE, Frostig RD, Hildesheim R. 1994. Cortical point-spread function and long-range lateral interactions revealed by real-time optical imaging of macaque monkey primary visual cortex. *J Neurosci* 14: 2545-68

Moreno-Bote R, Beck J, Kanitscheider I, Pitkow X, Latham P, Pouget A. 2014. Information-limiting correlations. *Nature neuroscience*

Nienborg H, Cumming BG. 2006. Macaque V2 neurons, but not V1 neurons, show choice-related activity. *J Neurosci* 26: 9567-78

Nienborg H, Cumming BG. 2009. Decision-related activity in sensory neurons reflects more than a neuron's causal effect. *Nature* 459: 89-U93

Osborne LC, Lisberger SG, Bialek W. 2005. A sensory source for motor variation. *Nature* 437: 412-6

Palmer C, Cheng SY, Seidemann E. 2007. Linking neuronal and behavioral performance in a reaction-time visual detection task. *J Neurosci* 27: 8122-37

Palmer CR, Chen Y, Seidemann E. 2011. Uniform spatial spread of population activity in primate parafoveal V1. *J Neurophysiol*

Pitkow X, Liu S, Angelaki DE, DeAngelis GC, Pouget A. 2015. How can single sensory neurons predict behavior? *Neuron* 87: 411-23

Purushothaman G, Bradley DC. 2005. Neural population code for fine perceptual decisions in area MT. *Nature Neuroscience* 8: 99-106

Ress D, Heeger DJ. 2003. Neuronal correlates of perception in early visual cortex. *Nature Neuroscience* 6: 414-20

Reynolds JH, Heeger DJ. 2009. The Normalization Model of Attention. *Neuron* 61: 168-85

Shoham D, Glaser DE, Arieli A, Kenet T, Wijnbergen C, et al. 1999. Imaging cortical dynamics at high spatial and temporal resolution with novel blue voltage-sensitive dyes. *Neuron* 24: 791-802

Sit YF, Chen Y, Geisler WS, Miikkulainen R, Seidemann E. 2009. Complex dynamics of V1 population responses explained by a simple gain-control model. *Neuron* 64: 943-56

Uka T, DeAngelis GC. 2004. Contribution of area MT to stereoscopic depth perception: choice-related response modulations reflect task strategy. *Neuron* 42: 297-310

Zohary E, Shadlen MN, Newsome WT. 1994. Correlated Neuronal Discharge Rate and Its Implications for Psychophysical Performance. *Nature* 370: 140-43

# Figure 1

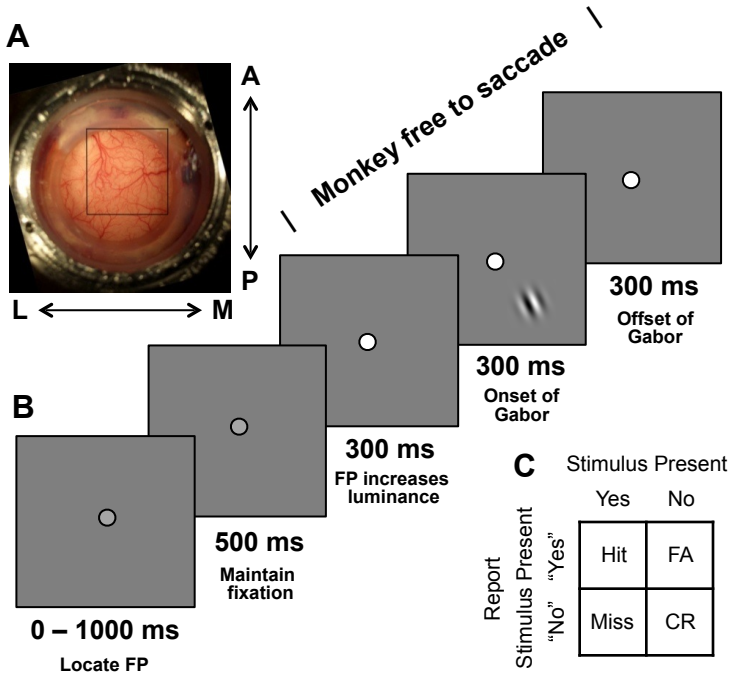


**Figure 1. Visual detection task and simultaneous VSDI recording**. **A**, cranial window over dorsal V1. Black square indicates VSDI imaging area of 10 x 10 $mm^2$ in the left hemisphere. Letters indicate approximate cortex orientation (A – anterior; P – posterior; M – medial; L – lateral). **B**, behavioral task. Each trial begins when the subject locates and fixates a central fixation point. After a 500 ms delay during which the subject is required to maintain fixation, the fixation point undergoes a slight increase in luminance to indicate the start of the task portion of the trial. Following a 300 ms delay, a Gabor stimulus appears on 50% of trials. The subject is required to make a saccadic eye movement to the stimulus location when it appears, or to maintain fixation on the central fixation point for an additional 900 ms when it does not appear. The subject receives a drop of juice or water following correct choices, and no reward following incorrect choices. **C**, a table with four possible behavioral outcomes.

# Figure 2

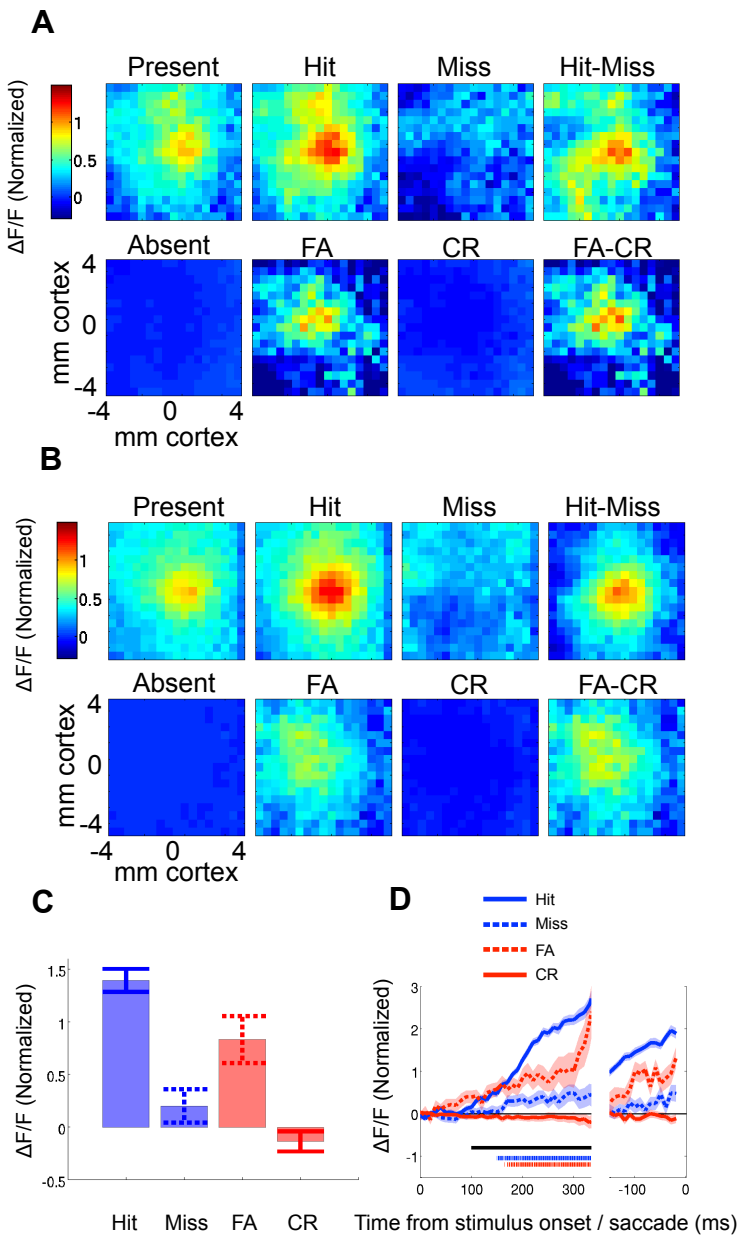


**Figure 2. Choice-related population activity in V1**. **A**, Example VSDI experiment in Monkey T. Average cortical activity maps separated by stimulus condition (rows) and behavioral choice (columns). Upper row of panel **A** represents neural activity during target-present trials; lower row shows activity during target-absent trials. Activity maps are shown separately for 'choose target-present' (Hit and FA) and 'choose target-absent' (Miss and CR) trials. 'Hit-Miss', difference map of activity during Hit and Miss trials. 'FA-CR', difference map of activity during FA and CR trials. Cortical maps represent activity averaged over the time interval indicated by the horizontal black bar in **D. B-D**, Aggregate summary of VSDI results collapsed over 22 experiments in Monkey T and 5 experiments in Monkey C. **B**, Same organization, space and time windows, and color scheme as in **A**. **C**, Bar plot showing the mean and SE (bootstrapped) of response amplitudes (computed over 2.5x2.5 $mm^2$ centered at the peak response) for each of the 4 behavioral categories. Means are weighted averages, with weights proportional to the SNR in each experiment. Bar plots were normalized for display such that the mean target-absent response was 0 and the mean target-present response was 1. **D**, Time evolution of mean response amplitudes for each of the 4 behavioral categories. Shaded areas indicate bootstrapped standard errors. Hash marks at the bottom of the panel indicate saccadic onset times in Hit (blue) and FA (red) trials. The left side of panel **D** shows responses aligned to stimulus onset; the right side of panel **D** shows responses aligned to saccadic eye movement onset. In the right side of panel **D**, traces for trials in which the monkey did not make an eye movement (Miss and CR trials) are shown for intervals re-sampled from those of the Hit and FA trials.

# Figure 3

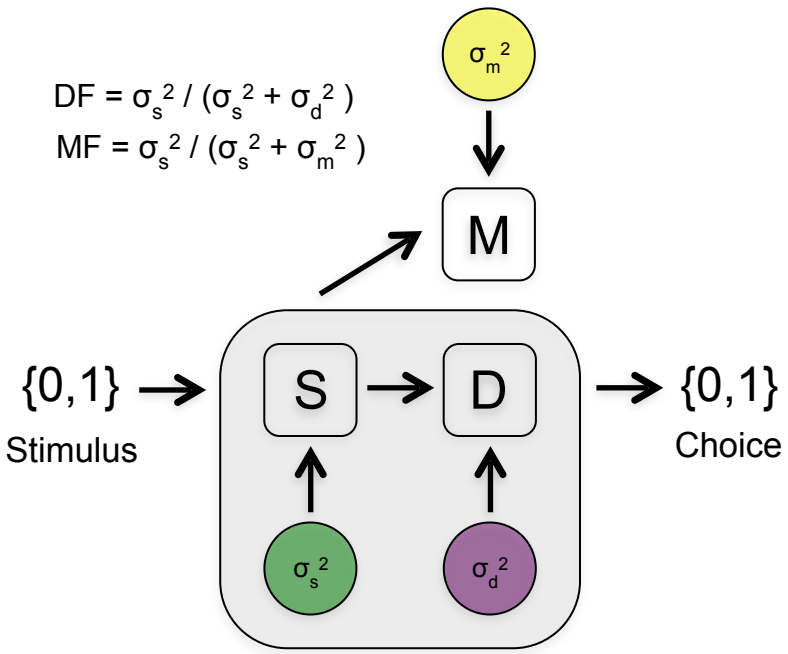


**Figure 3. Theoretical framework.** Model of a subject's formation of a binary decision and a researcher's measurement of neuronal responses. Stimulus-induced responses in an early sensory area come from distributions with means 0 and 1 and variance $\sigma_s^2$ (green). Zero-mean noise with variance $\sigma_d^2$ representing downstream variability (purple) is added to form the decision variable. The subject compares the decision variable to a criterion to form a decision on each trial. The upper portion of this panel represents stages in a researcher's measurement, in which zero-mean choice-unrelated noise with variance $\sigma_m^2$ (yellow) is added to the sensory representation to form the measured signals. The measured signals are then analyzed with respect to the subject's binary choices on a trial-by-trial basis.

# Figure 4

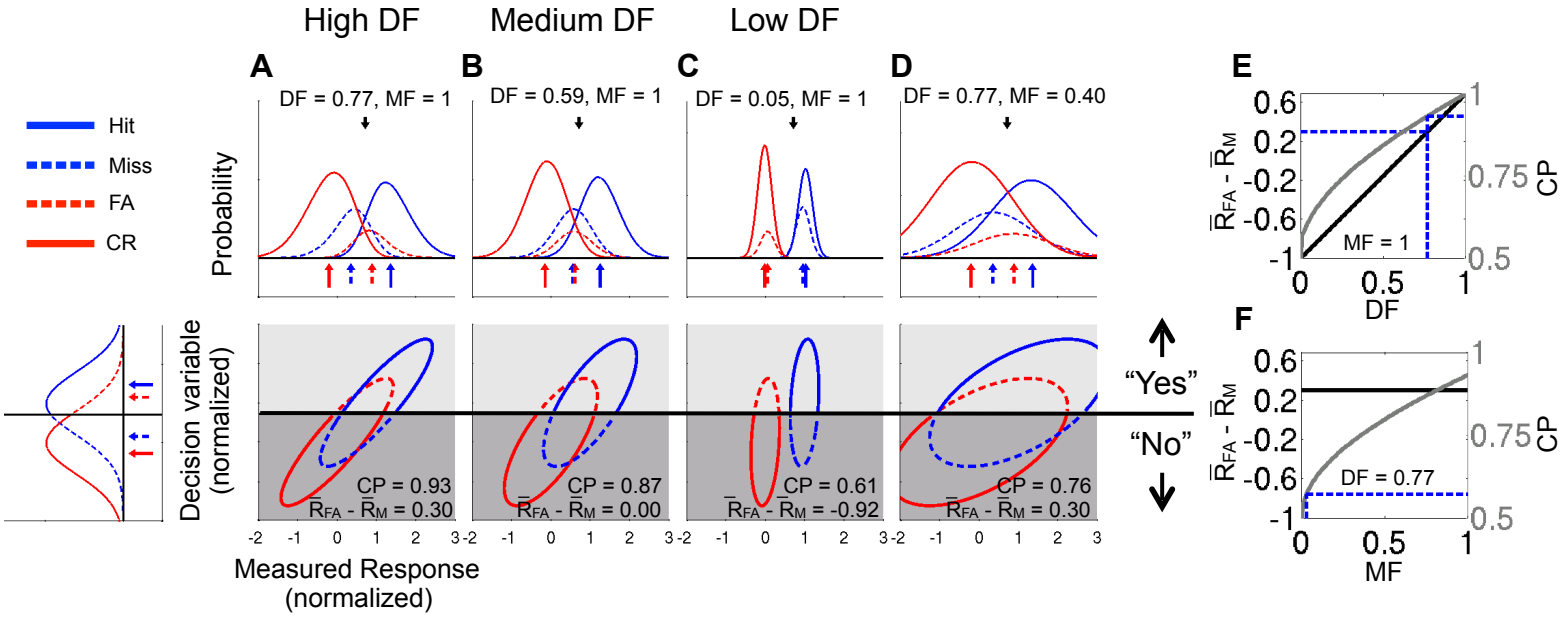


**Figure 4**. **Expected relationship between observable quantities and the underlying properties of a decision**. **A-D (lower)**, Joint distributions of the decision variable (ordinates) and model-predicted pooled neuronal responses (abscissae) under 4 noise scenarios, ranging from 77% of choice-related variability occurring in a measured brain area (**A**) to only 5% of choice-related variability captured by the measurement and the remaining 95% occurring downstream (**C**). In panels **A-D**, marginal distributions are shown for the four behavioral categories. The marginal distributions of the ordinate of panel **A** represent the decision variable which is controlled by the animal's overall accuracy and is therefore fixed in all panels. Red and blue arrows indicate mean neuronal response amplitude for each of the 4 behavioral categories. In panel **B**, the mean neuronal response amplitude for 'Miss' trials is identical to that of FA trials (dotted red arrow). Black arrows (top panels) and horizontal black lines (bottom panels) indicate the decision criterion. Mean response in FA minus mean response in Miss ($\bar{R}_{FA} - \bar{R}_M$), and choice probability (CP) values (see text for details) are reported for each scenario. In panels **A-C**, no choice-unrelated variability was added to the expected measured responses (i.e., MF = 1). **D**, Same as panel **A**, after adding a large amount of choice-unrelated variability. **E**, Relationship between $\bar{R}_{FA} - \bar{R}_M$ (left ordinate, black), CP (right ordinate, gray), and DF in the simplified model. Dotted blue lines indicate DF solution from the full model applied to the real data for the choice-triggered pooling rule in the absence of choice-unrelated noise (i.e., MF=1) and corresponding $\bar{R}_{FA} - \bar{R}_M$ and CP values in the simplified model. **F**, The relationship between $\bar{R}_{FA} - \bar{R}_M$ (left ordinate, black), CP (right ordinate, gray), and MF in the simplified model when DF = 0.77. While $\bar{R}_{FA} - \bar{R}_M$ is independent of MF, CP varies systematically with MF. Dotted blue lines indicate MF solution from the full model applied to the real data for the choice-triggered pooling rule (MF = 0.03) and corresponding CP value in the simplified model. The large amount of choice-unrelated variability reflects a combination of neural variability (e.g., independent neural variability that is captured by our measurements but does not affect choice) and non-neural measurement noise.

# Figure 5

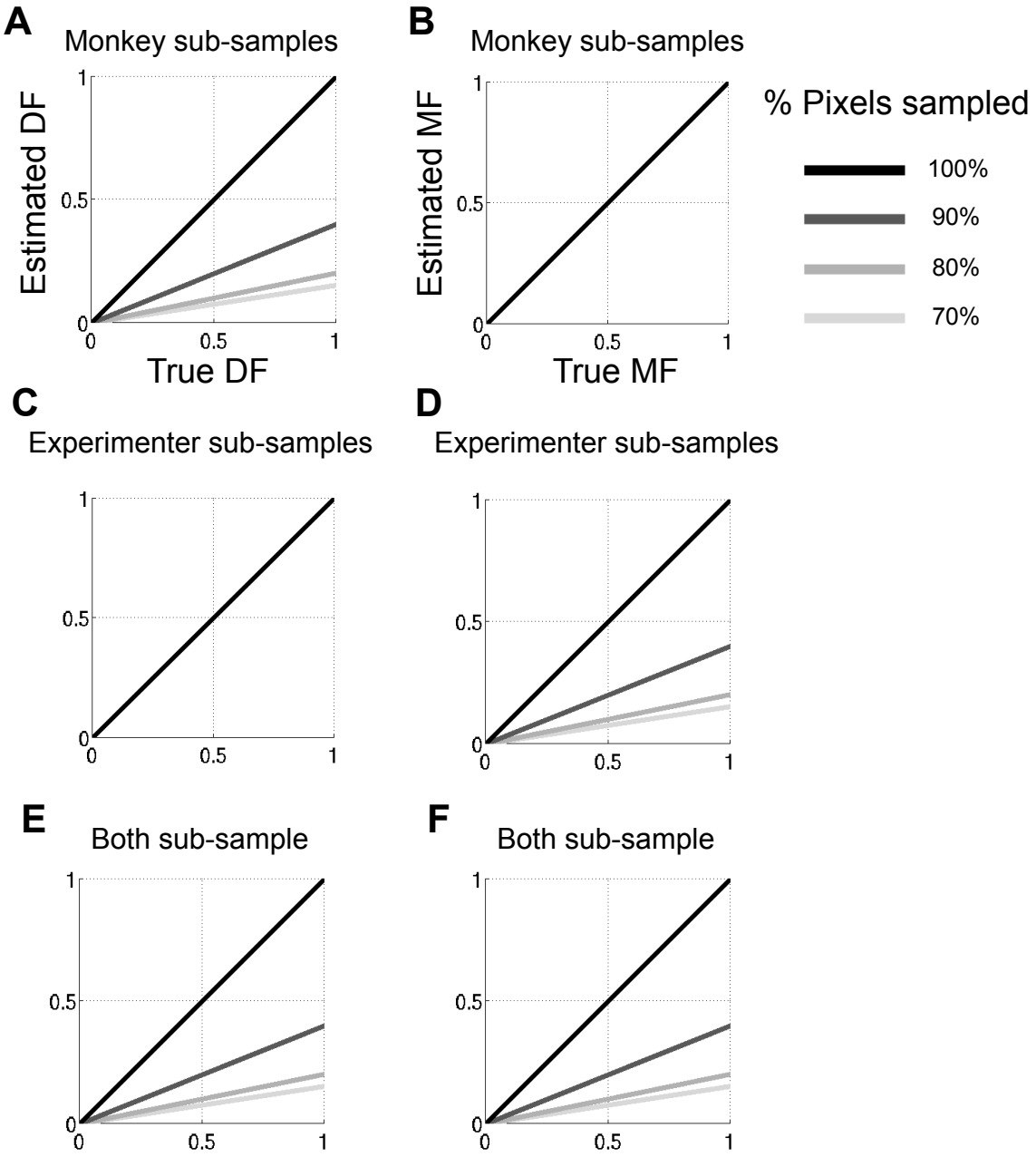


**Figure 5**. **Sub-sampling analysis**. Relationships between DF and MF values inferred using the maximum likelihood method (ordinates) and those used to generate the simulation (abscissae) during conditions in which the simulated monkey sub-samples the cortical population (**A,B**), the simulated experimenter sub-samples (**C,D**), and both the simulated monkey and experimenter sub-sample (**E,F**) (see Supplementary Methods). Black lines in **A-D** correspond to the case in which our initial assumption of equal access is met (see text for details). Grey lines indicate the percentage of pixels sampled. This figure demonstrates that the DF and MF values inferred with the maximum likelihood method provide lower bounds on their true values.

# Figure 6

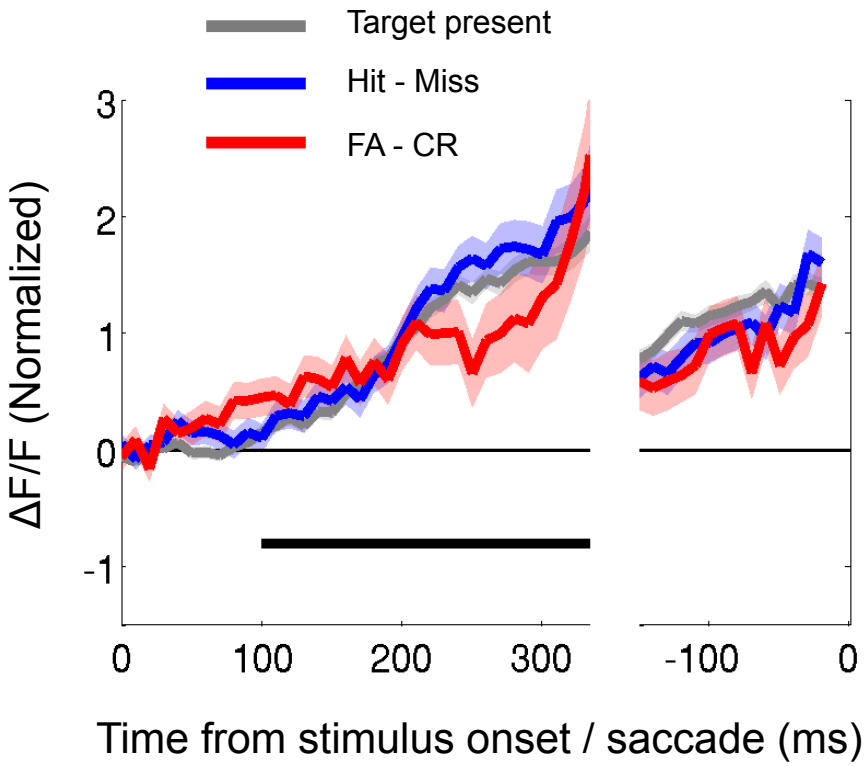


**Figure 6. Temporal dynamics of choice-related activity**. Time evolution of choice-related differences during target-absent trials (red, mean 'FA' minus mean 'CR' activity) and target-present trials (blue, mean Hit minus mean Miss activity) are shown alongside the time evolution of the stimulus-evoked response (grey). Shaded areas indicate standard errors. The near correspondence between the onset and dynamics of the choice-related signals and that of the stimulus-evoked response provides evidence against a *post-decisional* top-down mechanism in which we would expect the choice-related signals to manifest only well after the evoked response. Additionally, these temporal dynamics are dissimilar to those we observed in a recent study designed to directly test the effects of spatial attention in V1 in a similar detection task, in which we observed attentional effects that occurred shortly *before* stimulus onset and spread over a larger spatial extent than the stimulus evoked response (Chen & Seidemann 2012). Thus, the temporal dynamics of our choice-related modulations appear to be inconsistent with both a post-decisional top-down mechanism as well as a pre-decisional attention-like signal.

# Figure 7

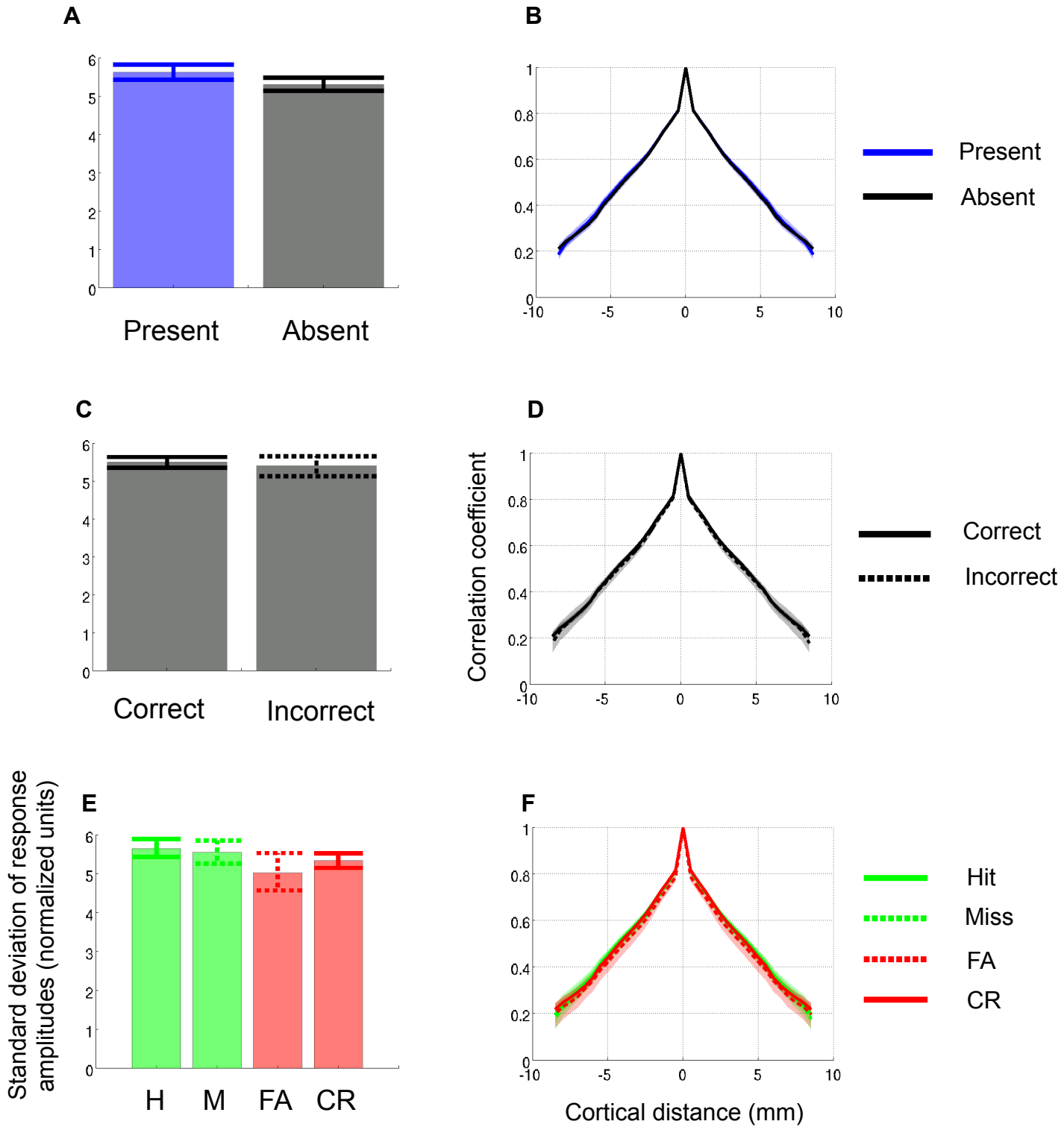


**Figure 7. Measured variability and noise correlations as a function of cortical distance**. (**A,C,E**) Standard deviations of normalized response amplitudes; (**B,D,F**) pixel-to-pixel correlation coefficients computed across all pairs of pixels, plotted as a function of cortical distance. Error bars and shaded areas indicated 95% confidence intervals (bootstrapped). The noise levels and spatial correlation profiles were statistically indistinguishable during target-present vs. target-absent trials (**A-B**), during correct vs. incorrect choices (**C-D**), and during each of the four behavioral outcomes (**E-F**).

# Table 1

| Pooling Model | DF | MF | CP (MF=1) | CP |
|---|---|---|---|---|
| 1 - Fitted Choice-triggered Average | 0.77 (0.56, 1.00) | 0.03 (0.01, 0.06) | 0.93 | 0.56 |
| 2 - Fitted Average Evoked | 0.77 (0.54, 1.00) | 0.03 (0.02, 0.06) | 0.93 | 0.56 |
| 3 - Gaussian (sigma=0.5 mm) | 0.97 (0.81, 1.00) | 0.07 (0.05, 0.11) | 0.99 | 0.61 |
| 4 - Gaussian (sigma=1 mm) | 0.96 (0.78, 1.00) | 0.06 (0.04, 0.10) | 0.99 | 0.60 |
| 5 - Gaussian (sigma=2 mm) | 0.86 (0.67, 1.00) | 0.04 (0.02, 0.07) | 0.96 | 0.58 |
| 6 - Gaussian (sigma=3 mm) | 0.77 (0.55, 1.00) | 0.03 (0.02, 0.06) | 0.93 | 0.56 |
| 7 - Gaussian (sigma=4 mm) | 0.72 (0.45, 1.00) | 0.03 (0.01, 0.06) | 0.92 | 0.56 |
| 8 - Optimal (Present v. Absent) | 0.98 (0.76, 1.00) | 0.05 (0.03, 0.09) | 0.99 | 0.59 |
| 9 - Optimal (“Yes” v. “No”) | 0.99 (0.79, 1.00) | 0.05 (0.03, 0.10) | 0.99 | 0.60 |

**Table 1. Model solutions for 9 alternative pooling rules.** We repeated our maximum likelihood estimation procedure (see Supplementary Methods) for each of 9 alternative candidate pooling rules to obtain estimates for DF and MF. DF estimates ranged from 0.72 to 0.99, and MF estimate ranged from 0.03 to 0.07 across pooling rules. For each pooling rule, we also computed choice probability expected under the simplified model associated with the DF and MF solutions. ‘CP (MF = 1)’ refers to the choice probability value associated with each pooling rule’s DF solution, in the absence of choice-unrelated noise (i.e., MF = 1). ‘CP’ refers to the choice probability value associated with each pooling rule’s DF solution, after the measured neural signals have been corrupted by the addition of choice-unrelated noise consistent with that pooling rule’s MF solution. Values in parentheses indicate 95% confidence intervals.